

Research Article

A New Method for Weak Fault Feature Extraction Based on Improved MED

Junlin Li,¹ Jingsheng Jiang,¹ Xiaohong Fan,² Huaqing Wang ,¹ Liuyang Song ,^{1,3} Wenbin Liu,¹ Jianfeng Yang,¹ and Liangchao Chen¹

¹School of Mechanical & Electrical Engineering, Beijing University of Chemical Technology, Chaoyang District, Beijing 100029, China

²College of Mechanical and Energy Engineering, Jimei University, Jimei District, Xiamen 361021, China

³Graduate School of Bioresources, Mie University, 1577 Kurimamachiya-cho, Tsu, Mie 514-8507, Japan

Correspondence should be addressed to Huaqing Wang; hqwang@mail.buct.edu.cn and Liuyang Song; xq-0703@163.com

Received 27 September 2017; Accepted 9 December 2017; Published 2 January 2018

Academic Editor: Sandris Ručevskis

Copyright © 2018 Junlin Li et al. This is an open access article distributed under the Creative Commons Attribution License, which permits unrestricted use, distribution, and reproduction in any medium, provided the original work is properly cited.

Because of the characteristics of weak signal and strong noise, the low-speed vibration signal fault feature extraction has been a hot spot and difficult problem in the field of equipment fault diagnosis. Moreover, the traditional minimum entropy deconvolution (MED) method has been proved to be used to detect such fault signals. The MED uses objective function method to design the filter coefficient, and the appropriate threshold value should be set in the calculation process to achieve the optimal iteration effect. It should be pointed out that the improper setting of the threshold will cause the target function to be recalculated, and the resulting error will eventually affect the distortion of the target function in the background of strong noise. This paper presents an improved MED based method of fault feature extraction from rolling bearing vibration signals that originate in high noise environments. The method uses the shuffled frog leaping algorithm (SFLA), finds the set of optimal filter coefficients, and eventually avoids the artificial error influence of selecting threshold parameter. Therefore, the fault bearing under the two rotating speeds of 60 rpm and 70 rpm is selected for verification with typical low-speed fault bearing as the research object; the results show that SFLA-MED extracts more obvious bearings and has a higher signal-to-noise ratio than the prior MED method.

1. Introduction

Rolling bearings are one of the most widely used elements in rotary machines. The mechanical failure of bearings may result in financial loss, and even death. Therefore, condition monitoring and fault diagnosis of rolling bearings are critically important for production efficiency and plant safety in modern enterprises [1, 2]. When a rolling bearing fault is weak at an early stage or at a low shaft speed, weak fault features are often embedded in background noise. So it is not an easy task to extract the representative features from the original signal [3]. For instance, the fast Fourier transform cannot obtain ideal transient extraction, even as an increased signal-to-noise ratio assists weak fault feature extraction. Many scholars have reviewed the problem of fault diagnosis taken from weak signals and have made progress. In [4], wavelet transformation is applied to the problem of weak, abnormal vibration signal extraction, but reliance

upon a single wavelet transform makes the extraction of complex vibration signals difficult [5, 6]. Many approaches to improved wavelet transform signal extraction have been proposed, by combination with other diagnostic tools: neural networks, hidden Markov models, or singular value decomposition. In some cases, good results were obtained, but these approaches require the setting of a great many parameters, and yet when the signal is quite weak or the noise strong, these approaches give poor results [7–10]. Huang et al. in 1998 proposed empirical mode decomposition (EMD), an adaptive signal processing method that yields intrinsic mode functions (IMFs) [11]. EMD algorithms are widely used for rolling bearing fault type identification. However, there is a serious pattern mixing and endpoint effect in the EMD method. Wu and Huang proposed ensemble empirical mode decomposition (EEMD) to overcome the shortcoming of mode mixing, but end effects remain a problem. So the

EMD and EEMD methods cannot be qualified for weak fault diagnosis [12, 13]. Stochastic resonance is usually used to enhance weak fault signals and to extract rolling bearing characteristic frequency components [14, 15]. Given the difficulty of choosing the parameters of a band-pass filter, spectral kurtosis (SK) is another useful tool; it provides a moderate way of detecting weak fault in rotation even under the background of strong noise [16, 17]. Liu et al. put forward a new method to extract new features using kernel joint approximate diagonalization of eigenmatrices (KJADE) [18]. Sparse decomposition derived from application of a matching pursuit algorithm to fault signal data can detect the amplitude, the frequency, and the phase of weak signals under the background of strong noise [19]. These results are not obvious because of the loss of signal details.

Wiggins introduced minimum entropy deconvolution (MED) in 1978. MED has been applied to seismic signal processing, especially for the separation of convolutional components of reflection signals [20]. In 2007, Sawalhi et al. first applied MED to detection of faults in rolling bearings and other gear. MED is usually combined with spectral kurtosis or AR filtering to enhance rolling bearing fault detection and diagnosis [21, 22]. MED is also a valid approach to the period estimation problem [23]. However, given strong noise, the failure impact component will be lost by MED, and this is because of the following reasons [24–26].

MED is used as a linear operator and so is ill-adapted to process a limited frequency bandwidth. For noisy data, the limitation of the linear operator is difficult to overcome.

The filter coefficients obtained by the objective function method (OFM) are local optima, not global optima.

To address the latter limitation, an improved MED method based on the shuffled frog leaping algorithm (SFLA-MED) is proposed. In the new method, a shuffled frog leaping algorithm (SFLA) is applied to select an optimal set of filter coefficients that provide maximum kurtosis. So, the filtered signal will be acquired by taking advantage of a global optimal inverse filter. The envelope spectrum of the filtered signal is calculated with Hilbert transform (HHT) and fast Fourier transform (FFT). In the envelope spectrum, the characteristic frequency of a rolling bearing is quite obvious, and the bearing faults can be diagnosed.

2. Overview of the Improved Algorithm

2.1. Minimum Entropy Deconvolution Algorithm. Deconvolution is an inverse filter that is typically applied to seismic data, for the purpose of recovering reflection coefficients. The main benefit is compression of the seismic reflection pulse and to improve estimation of the subsurface reflection interface reflection coefficient. Deconvolution is particularly important to the bright spot technique of oil-gas exploration and to the analysis of seismic data associated with lithological study on the formation of seismology. Deconvolution can remove the interference from short cycle reverberation and multiple waves [27, 28]. Deconvolution can be divided into deterministic deconvolution and predictive deconvolution. There are many commonly known deconvolutions, including

east square deconvolution, predictive deconvolution, homomorphic deconvolution, surface-consistent deconvolution, maximum entropy deconvolution, minimum entropy deconvolution, change mould deconvolution, Q deconvolution, Noah deconvolution, and minimum information deconvolution.

The MED technique is a type of system identification method that was originally developed to aid extraction of reflectivity information in seismic data. The reflectivity information can be used to identify and locate layers of subterranean minerals [23]. The essence of the method is to acquire a linear operator that maximizes the characteristics of the spike pulse [29, 30]. Maximum kurtosis defines a stop condition [30].

Rolling bearing fault vibration signal can be expressed as

$$y(n) = h(n) * x(n) + e(n), \quad (1)$$

where $x(n)$ is the impact sequence of the rolling bearing vibration signal, $h(n)$ is the transfer function, and $e(n)$ is the noise component. To facilitate analysis, $e(n)$ can be ignored. The purpose of MED is to find a deconvolution optimal inverse transfer function $f(n)$ to calculate an input signal $x(n)$ from the output signal $y(n)$ through (*).

$$x(n) = f(n) * y(n). \quad (*)$$

From (3) one may find the best inverse filter that maximizes the kurtosis index of original signal.

$$o_2^4(f(n)) = \frac{\sum_{i=1}^N x^4(i)}{[\sum_{i=1}^N x^2(i)]^2} \quad \text{that is} \quad \frac{\partial o_2^4(f(n))}{\partial f(n)} = 0. \quad (**)$$

Therefore, MED makes the recovery of signal by construction of an “optimal” filter possible.

MED can be summarized in five steps [26]:

(1) Initialization:

$$f^{(0)} = 1. \quad (***)$$

(2) Iteration computing:

$$x(n) = f(n)^{(i-1)} * y(n). \quad (2)$$

(3) Calculate the cross-correlation:

$$b^{(i)}(l) = a \sum_{n=1}^N x^3(n) y(n-l). \quad (3)$$

(4) Calculate the coefficient of filtering:

$$f^{(i)} = A^{-1} b^{(i)}. \quad (4)$$

(5) Terminate condition.

Assume that the given threshold is 0.01. If $\|f^{(i)} - f^{(i-1)}\|_2^2 < 0.01$, the iteration ends; else $i = i + 1$, and iterate.

2.2. Shuffled Frog Leaping Algorithm. SFLA combines the global breadth search of the entire frog populations and the local depth search of frogs individual information, leading the algorithm towards the global optimum direction [25, 31]. The frog representing the solution is divided into several subgroups, and each population has its own culture. Then the frogs evolve according to fitness in the population. After searching in each memplex, the frogs from all memplexes are shuffled and then frogs are redistributed forming new memplexes, which makes searching process less possible to be trapped in local optimum [31].

Its steps include the following:

- (1) Initialize population size.
- (2) Initialize population generation $U(i)$; calculate the $U(i)$ performance of $f(i)$:

$$U(i) = (U_i^1, U_i^2, \dots, U_i^d). \quad (5)$$

- (3) Rank the frogs $U(i)$, and arrange the array according to $f(i)$:

$$X = \{U(i), f(i), i = 1, 2, \dots, F\}. \quad (6)$$

- (4) The frogs $U(i)$ are placed in different populations in turn.
- (5) Within populations, frogs begin to evolve (update the worst frogs in the population):

$$Di = \text{rand}() * (Pb - Pw). \quad (7)$$

- (6) After the evolution of the population, the subgroups are combined and arranged in descending order. By constantly iterating, then find out the best frogs to update.

The output signal of a linear time invariant system (LTI) system can be expressed as follows:

$$y(n) = \sum_{i=0}^{N-1} b_i x(n-i) - \sum_{i=1}^M a_i y(n-i). \quad (*a)$$

$x(n)$ is the input signal, a_i and b_i represent filtering coefficients, and N is the filter order. In this paper, $a_i = 0$,

$$y(n) = \sum_{i=0}^{N-1} b_i x(n-i). \quad (*b)$$

The best filter coefficient (f_i) obtained by the leapfrog algorithm is substituted into the formula (*b); then the denoising signal $x'(n)$ becomes

$$x'(n) = \sum_{i=0}^{N-1} f_i x(n-i). \quad (*c)$$

Then the denoising signal $x'(n)$ is demodulated by HILBERT-FFT envelope. Finally, the validity of SFLA-MED is verified by comparing the envelope spectrum with the fault characteristic value.

2.3. Diagnosis Method by the SFLA-MED. Figure 1 shows the differences between MED and the SFLA-MED. The MED filter is implemented by the objective function method (OFM) given in reference [26]. The OFM is an optimization process designed to maximize the kurtosis of the MED output. It is pointed out that the filter coefficients obtained by OFM are merely local optima, not global optima. So the SFLA-MED uses SFLA to find these optimal coefficients.

The process of fault diagnosis is shown in Figure 2. Vibration signals are measured in a low-speed bearing experiment. The SFLA-MED method does not need to set threshold parameters during the iteration and directly filters the original signal so that a new signal formed. Envelope demodulation is then applied to the new signal. Envelope demodulation consists of a Hilbert transform (HHT) and a fast Fourier transform (FFT). To further verify the reliability and feasibility, the proposed method is compared to MED and theoretical characteristic frequency.

3. Experimental Validation

3.1. Simulation Signal Analysis. Assume the expression of the bearing simulation signal:

$$x(t) = s1 \times (1 + \cos(2\pi F_{r1}t) + \cos(2\pi F_{r2}t)) \times \cos(2\pi F_n t) + s2 \times \text{randn}(\text{size}(t)). \quad (* * a)$$

$s1$ is the amplitude of the shock component; the value was set to 1.5. The characteristic frequency $F_{r1} = 12$ Hz, $F_{r2} = 30$ Hz, and carrier frequency $F_n = 150$ Hz. The noise component is $\text{randn}(\text{size}(t))$, amplitude was 0.2. The time-domain waveform is shown in Figure 3.

Hilbert-FFT was used to demodulate the signals obtained by the MED method and the SFLA-MED method, and then the amplitude of the frequency domain was normalized for a clear contrast. As can be seen from Figure 4(a), after the signal had been reduced and processed by the MED method, the characteristic frequency was drowned in the noise signal, which cannot accurately extract the fault characteristics of the bearing. After the SFLA-MED method was adopted, the signal can be accurately extracted with 12 Hz and 30 Hz, and the harmonic characteristics were obvious, as shown in Figure 4(b). In addition, as can be seen from Figure 3, the modulation characteristics of the simulation signal were obvious, so the envelope analysis was carried out here, as shown in Figure 4(c). After the signal was enveloped, the submerged feature of the mixed white noise was well detected. It should be pointed out that the noise contained in the actual bearing fault signal was usually rather complicated. So the paper uses the method of SFLA-MED and envelope analysis to detect the weak fault signal of bearing.

3.2. Experimental Verification of Low-Speed Bearings

3.2.1. Experimental System. The experimental signals to be analyzed were collected from low-speed bearing experiments as shown in Figure 5. In order to better verify the effectiveness of the method put forward in this paper, the outer-race fault data and inner-race fault data of a rolling bearing were taken,

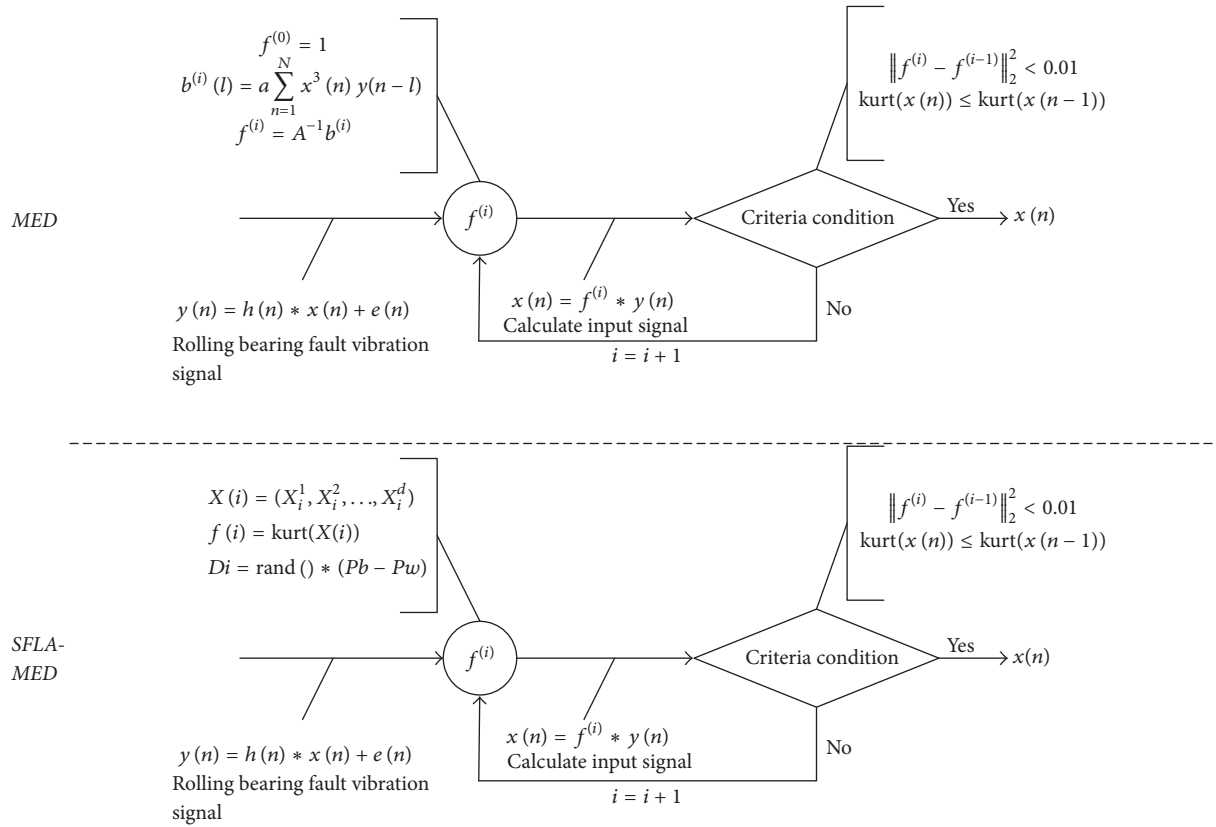


FIGURE 1: The calculation process of MED and the SFLA-MED.

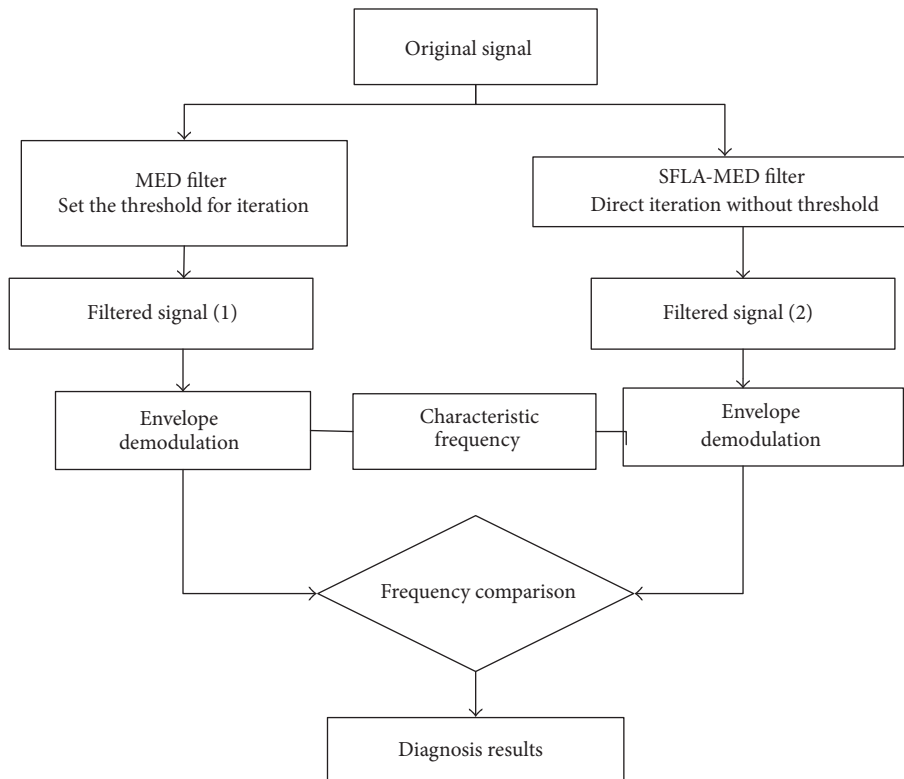


FIGURE 2: The flowchart of fault diagnosis.

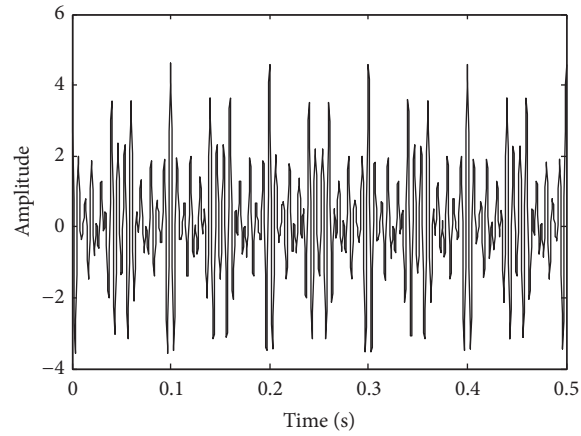


FIGURE 3: Time-domain waveform of simulation signal.

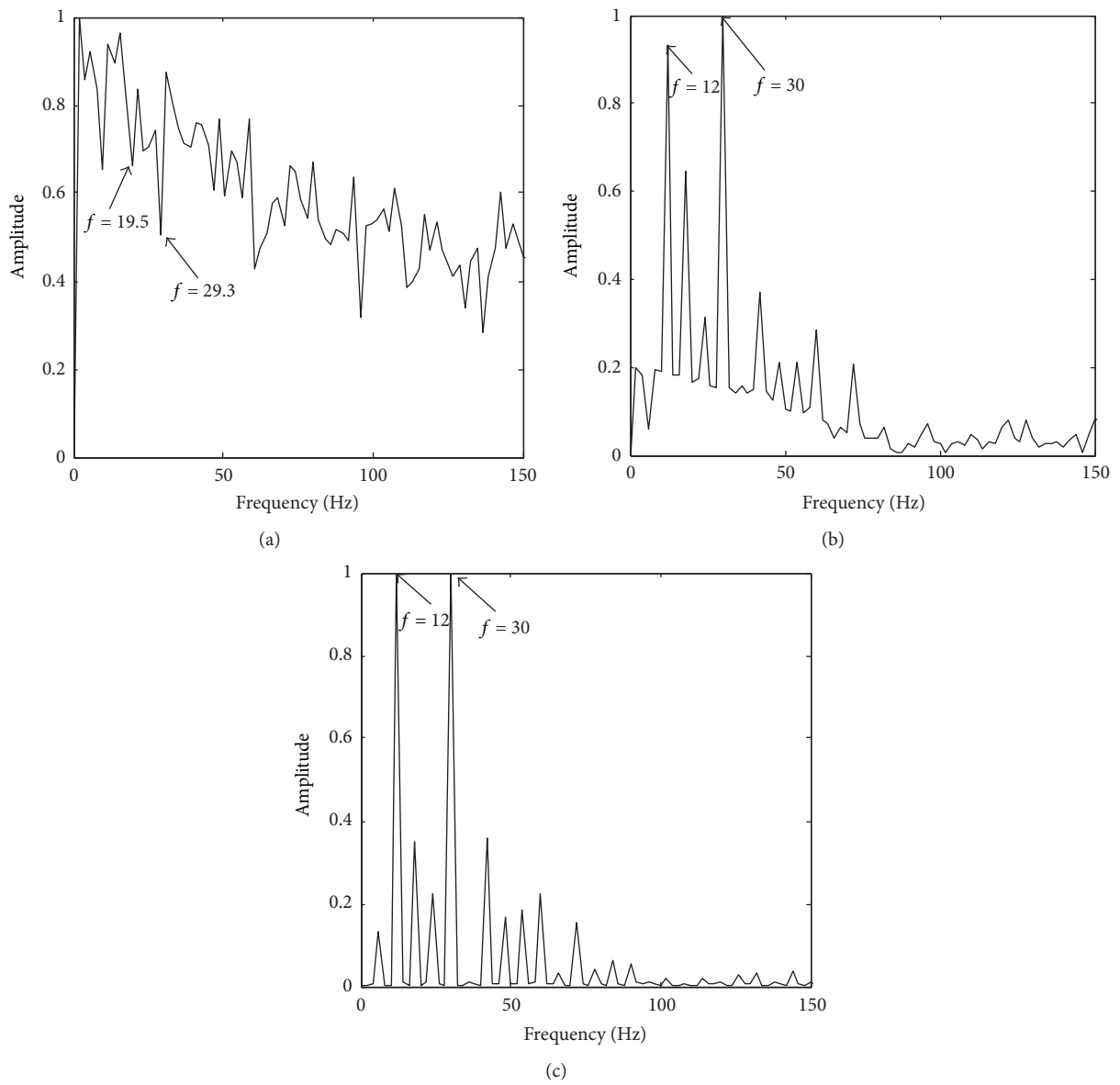


FIGURE 4: Diagnostic results of simulated signals. (a) MED method detection; (b) SFLA-MED method detection; (c) Hilbert-FFT method detection.

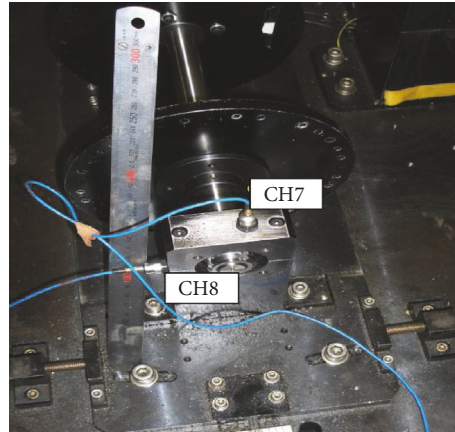


FIGURE 5: Low-speed bearing experimental system.



FIGURE 6: Fault bearings. (a) Outer-race fault; (b) inner-race fault.

and those flaws were artificially made with the use of a wire-cutting machine as shown in Figure 6. The sizes of the flaws are as follows:

Outer-race flaw: 5.0 mm * 0.5 mm (width * depth)

Inner-race flaw: 5.0 mm * 0.5 mm (width * depth).

3.2.2. Bearing Data Set Description. In order to fully analyze signal features and acquire more comprehensive information for the research of the fault diagnosis, the sampling frequency is set at 100 kHz, the sampling time is 10 seconds, and the rotation speed of spindle is 60 rpm and 70 rpm. So four kinds of vibration signal are obtained and they are outer-race fault vibration signal at 60 rpm, inner-race fault vibration signal at 60 rpm, outer-race fault vibration signal at 70 rpm, and the inner-race fault vibration signal at 70 rpm, respectively. By varying rotation speed, the time-domain wave form of vibration signals is shown in two figures. Figure 7 indicates the time-domain wave form of outer-race and inner-race fault vibration signals when the rotation speed is 60 rpm and Figure 8 shows the time-domain waveform of outer-race

and inner-race vibration signals when the rotation speed is 70 rpm.

Bearing defects will generate a series of impact vibrations that emit at bearing characteristic frequencies every time a running roller passes over a defect [32]. Therefore the fault type can be determined by identifying the characteristic frequency [33].

Computed pass-frequencies are shown in Table 1. Pure rolling motion is a condition of the above equations. As there may be some sliding motion in practice, the results in Table 1 are approximate values.

4. Results and Discussion

4.1. Feature Extraction of MED and SFLA-MED. Envelop spectrum analysis based on the Hilbert transform has been widely used in bearing fault diagnosis [34]. It separates modulating signal from the collected signal, and this contains information that indicates the fault type. Envelope spectrum analysis is obtained from the FFT of the envelop signal. Figure 9 shows the normalized envelop spectrum of outer-race and

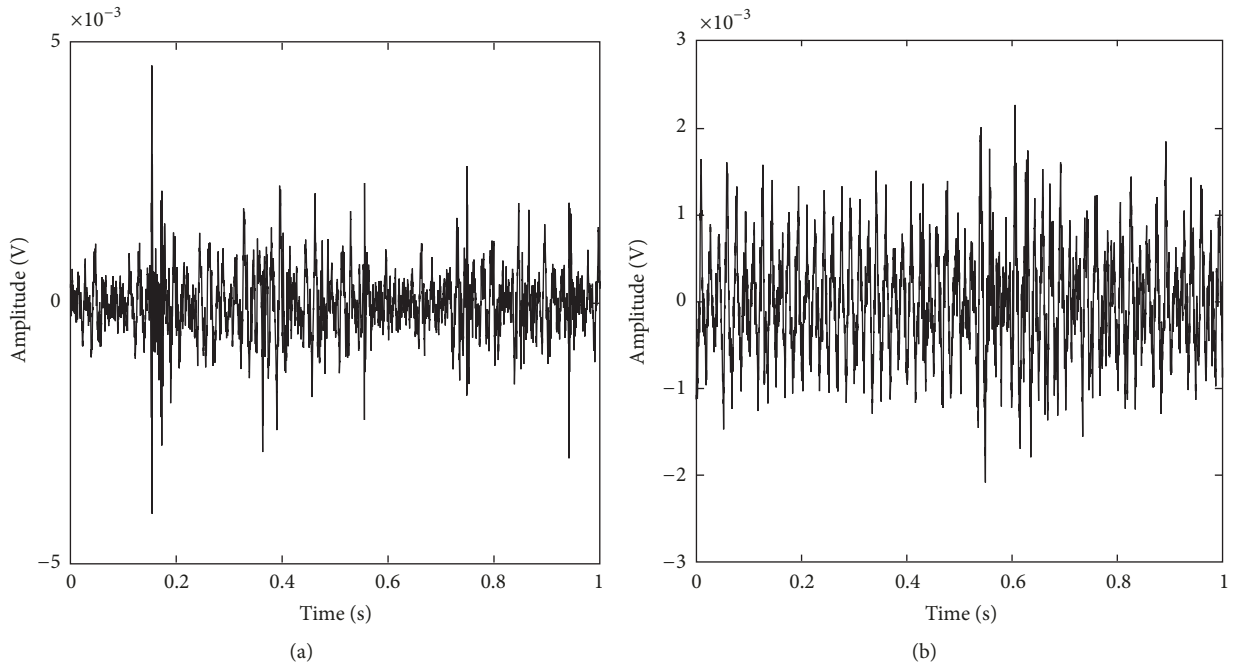


FIGURE 7: The time-domain waveform of vibration signals (60 rpm): (a) outer-race fault; (b) inner-race fault.

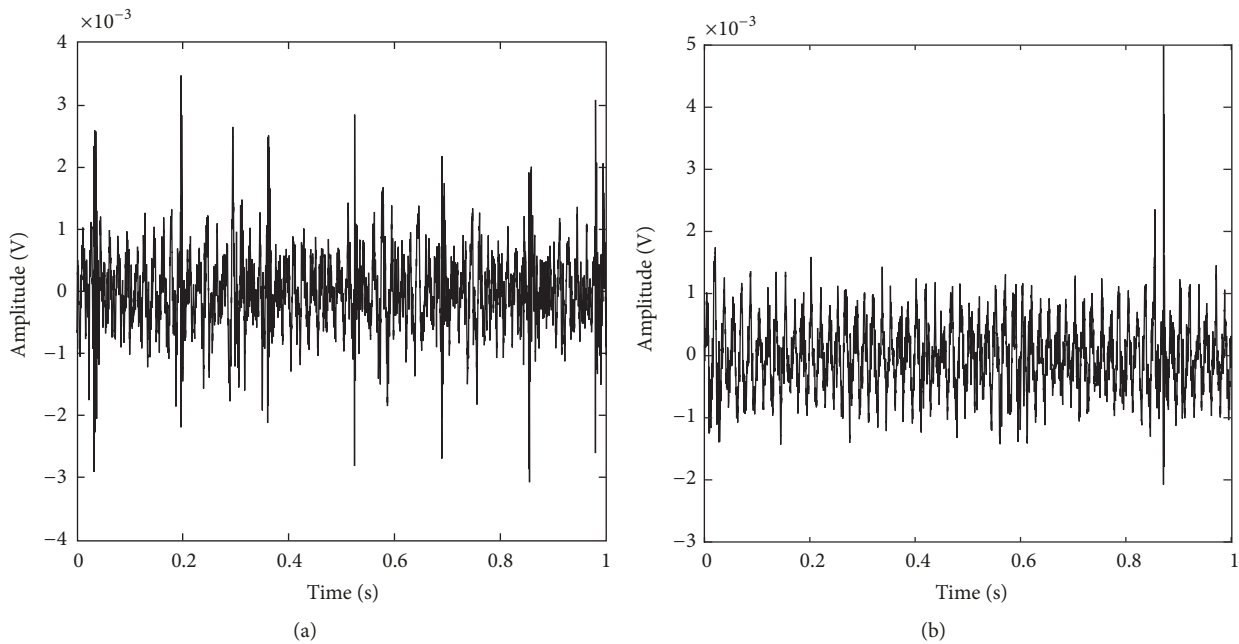


FIGURE 8: The time-domain waveform of vibration signals (70 rpm): (a) outer-race fault; (b) inner-race fault.

inner-race fault vibration signals at the speed of 60 rpm filtered by MED method. As shown in Figure 9(a), the theoretical characteristic frequency is not clearly shown by the spectrum peaks. Although there is a clear spectrum peak appearing near the theoretical characteristic frequency as shown in Figure 9(b), it is not the highest spectral peak and cannot be identified for the first time. Hence, the MED method extracts the fault characteristic frequency with contingency.

Shuffled Frog Leaping Algorithm optimization improves the MED method. Based on theoretical study, the frequency equation of bearing fault characteristics is based on the assumption of a pure rolling motion. These vibrations occur at bearing characteristic frequencies, which are estimated based on the geometry of the bearing, its rotational speed, and the location of the defect. However, in practice, some unexpected status may occur, which causes slight deviation

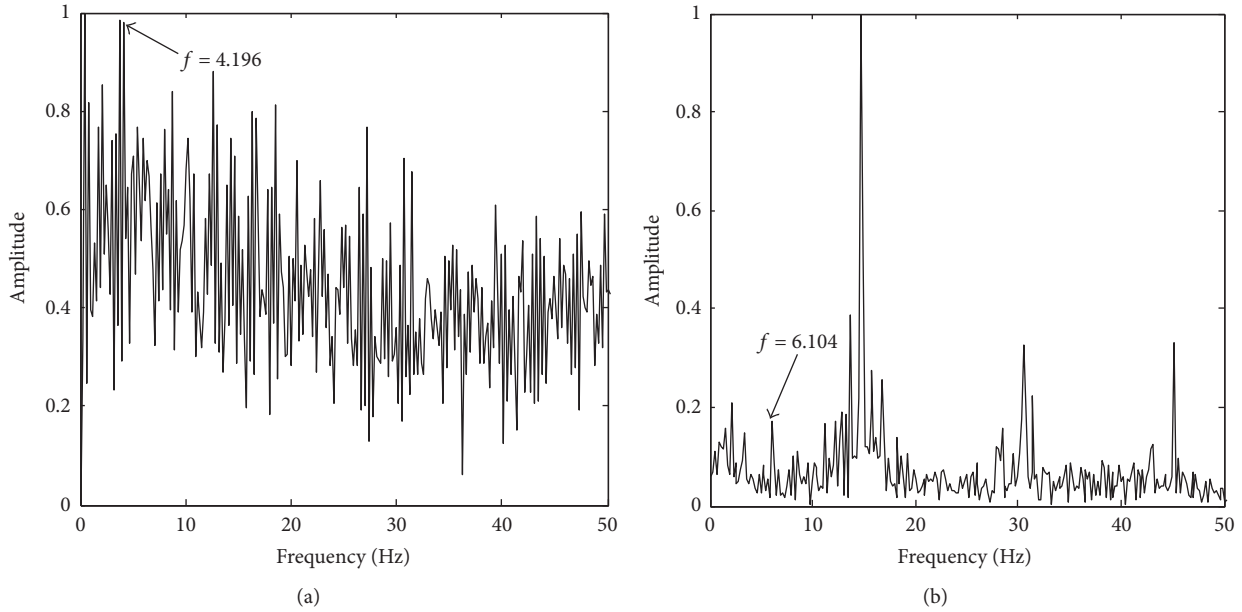


FIGURE 9: The envelope spectrum of vibration signals filtered by MED (60 rpm): (a) outer-race fault; (b) inner-race fault.

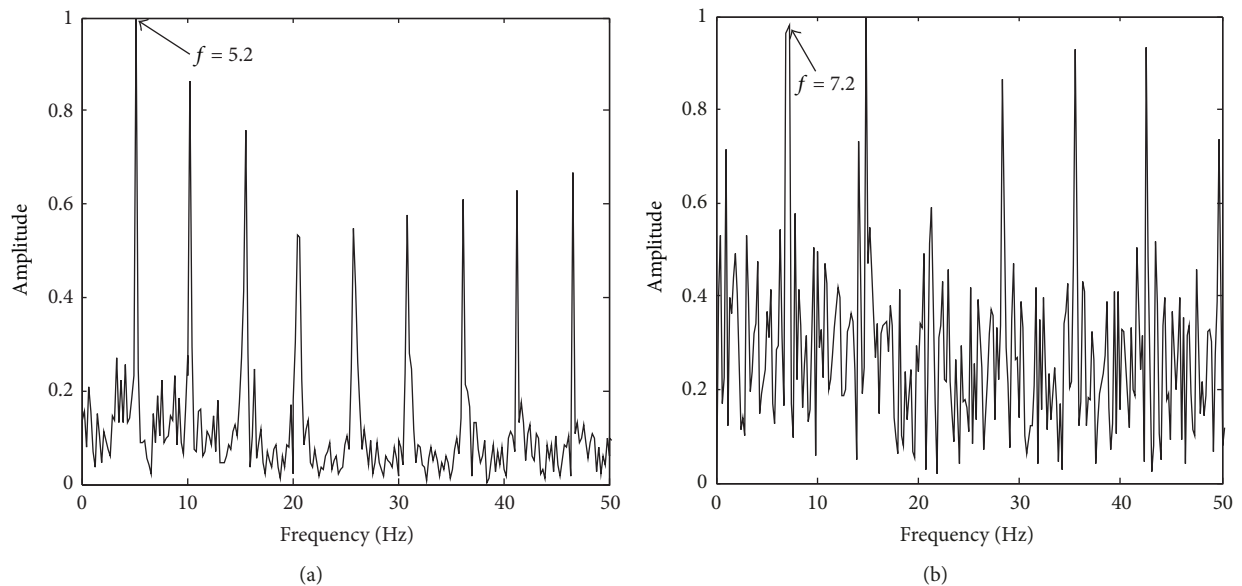


FIGURE 10: The envelope spectrum of vibration signals filtered by SFLA-MED (60 rpm): (a) outer-race fault; (b) inner-race fault.

of the characteristic frequency locations. Figure 10 shows the normalized envelop spectrum of outer-race and inner-race fault vibration signals at the speed of 60 rpm filtered by SFLA-MED. From Figure 10, it can be seen that there is an obvious spectrum peak corresponding to the theoretical characteristic frequency, so the results obtained from SFLA-MED meet the diagnostic accuracy requirement. In summary, the SFLA-MED method can better extract the fault characteristic frequency.

According to the experimental results in Figure 11, the traditional MED method can recognize the bearing failure, which shows the effectiveness of the MED method. The

SFLA-MED are used to analyze the experimental data, and it can also identify bearing failure, as shown in Figure 12. The two methods are good to identify fault bearing fault characteristics under 70 rpm. Compared with the 60 rpm experimental data, the SFLA-MED algorithm recognizes the characteristic frequency of the bearing fault under different speeds, which shows that it has a better universality and is more suitable for application.

4.2. Effect Comparison of MED and SFLA-MED. As is known, signal-to-noise ratio (SNR) is one of the most basic indicators to measure an algorithm. Combining the experimental data

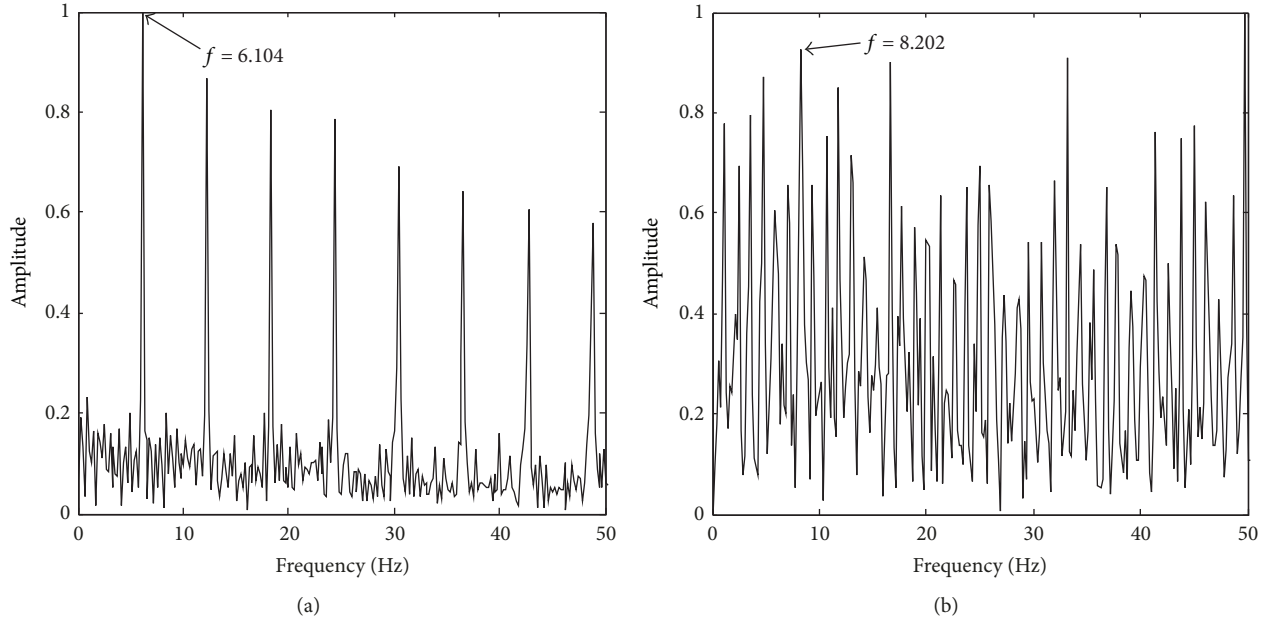


FIGURE 11: The envelope spectrum of vibration signals filtered by MED (70 rpm): (a) outer-race fault; (b) inner-race fault.

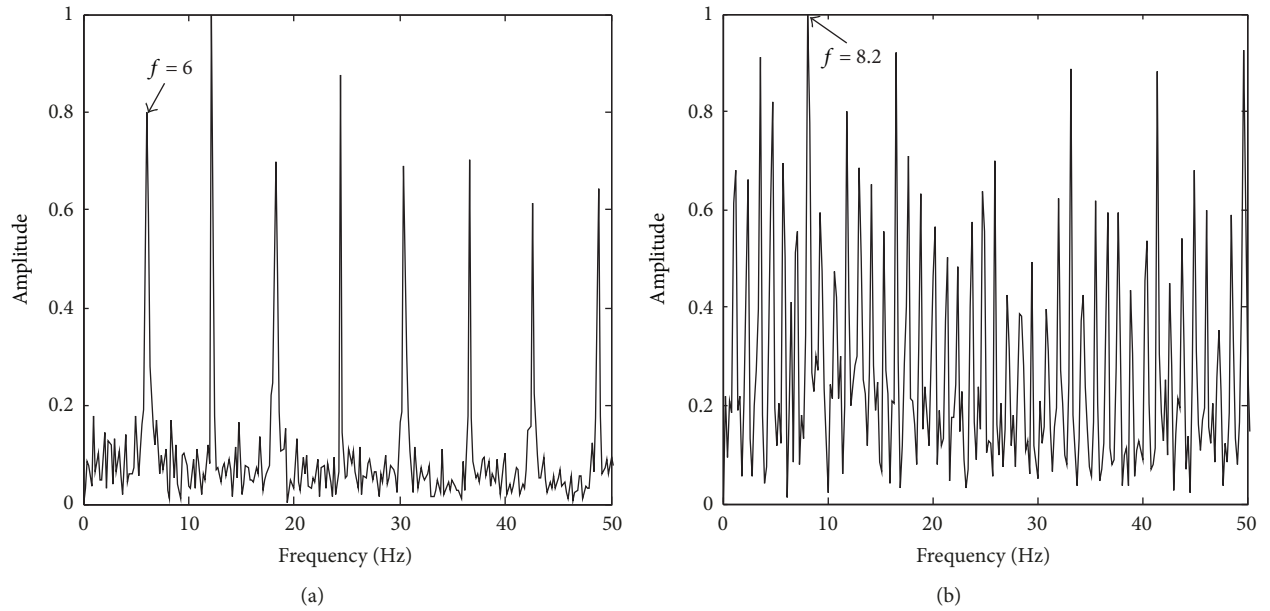


FIGURE 12: The envelope spectrum of vibration signals filtered by SFLA-MED (70 rpm): (a) outer-race fault; (b) inner-race fault.

of the four groups, it is found that the characteristic frequency signals of the SFLA-MED method are not drowned by noise, and they are more easily identified with the fault characteristics (highest spectrum peaks). In addition, compared with the experimental result of signals at the speed of 60 rpm, the SFLA-MED method has higher signal-to-noise ratio than the original MED method as shown in Table 2. Therefore, the SFLA-MED can extract the failure frequency more accurately and reduce the possibility of miscalculation.

The calculation formula of frequency domain signal-to-noise ratio is shown in.

$$R = \lg \frac{\sum_{r=1}^3 A_{F_r}^2}{\sum_{i=1}^N A_i^2 - \sum_{r=1}^3 A_{F_r}^2}. \quad (***)$$

N is the sampling length, A_{F_r} is the corresponding amplitude of the first three-order characteristic frequency, and A_i is the frequency domain signal amplitude.

TABLE 1: Pass-frequencies of rolling bearing.

Rotation speed	60 rpm	70 rpm
Outer-race fault	4.91 (Hz)	5.73 (Hz)
Inner-race fault	7.09 (Hz)	8.27 (Hz)

TABLE 2: SNR of two methods (dB).

	60 rpm Inner-race	60 rpm Outer-race
MED	-0.4814	-0.8050
SFLA-MED	-0.2691	1.8908

5. Conclusions

In this paper, an SFLA-MED combined with envelope demodulation is applied to the weak fault diagnosis of rolling bearings. Compared with the previous MED method, the proposed method extracts more obvious fault features of rolling bearings and is better adapted to engineering application. It is pointed out that the improved MED obtains a global optimal solution but that MED does not. SFLA makes the selection of filtering coefficients more flexible. As can be seen from the algorithm flow diagram, there is no error accumulation in the SFLA-MED, because the process of finding filter coefficients is not affected by the last filtered signal. There are no extra frequency components beyond the characteristic frequency that appears in the envelope spectrum.

Conflicts of Interest

The authors declare that there are no conflicts of interest regarding the publication of this paper.

Authors' Contributions

The presented work was carried out by collaboration of all authors. Huaqing Wang conceived and designed the experiments; Junlin Li and Jingshen Jiang performed the experiments and the simulations; Xiaohong Fan and Liuyang Song analyzed the data; Wenbin Liu, Jianfeng Yang, and Liangchao Chen performed the simulation and revised the paper; Junlin Li and Huaqing Wang wrote the paper. All authors read and approved the final manuscript.

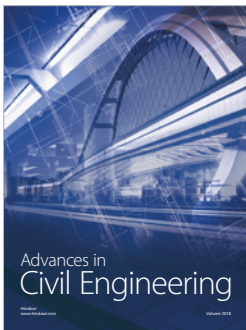
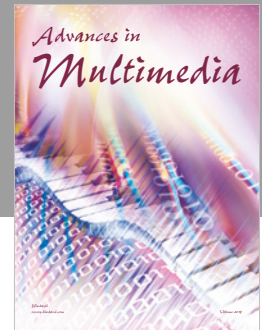
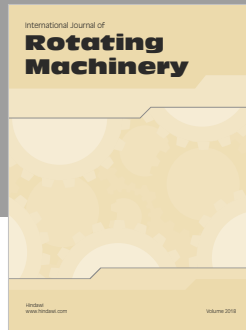
Acknowledgments

This paper is supported by the National Natural Science Foundation of China (Grant no. 51675035) and Petro-China Science and Technology Innovation Fund (Grant no. 2015D50060606).

References

- [1] N. Tandon and A. Choudhury, "Review of vibration and acoustic measurement methods for the detection of defects in rolling element bearings," *Tribology International*, vol. 32, no. 8, pp. 469–480, 1999.
- [2] J. Wang, L. L. Cui, H. Q. Wang, and P. Chen, "Improved complexity based on time-frequency analysis in bearing quantitative diagnosis," *Advances in Mechanical Engineering*, vol. 2013, Article ID 258506, 11 pages, 2013.
- [3] P. D. McFadden and J. D. Smith, "Vibration monitoring of rolling element bearings by the high-frequency resonance technique—a review," *Tribology International*, vol. 17, no. 1, pp. 3–10, 1984.
- [4] R. B. Randall and J. Antoni, "Rolling element bearing diagnostics—a tutorial," *Mechanical Systems and Signal Processing*, vol. 25, no. 2, pp. 485–520, 2011.
- [5] Z. K. Peng, P. W. Tse, and F. L. Chu, "A comparison study of improved Hilbert-Huang transform and wavelet transform: application to fault diagnosis for rolling bearing," *Mechanical Systems and Signal Processing*, vol. 19, no. 5, pp. 974–988, 2005.
- [6] X. S. Lou and K. A. Loparo, "Bearing fault diagnosis based on wavelet transform and fuzzy inference," *Mechanical Systems and Signal Processing*, vol. 18, no. 5, pp. 1077–1095, 2004.
- [7] H. C. Wang, J. Chen, and G. M. Dong, "Feature extraction of rolling bearing's early weak fault based on EEMD and tunable Q-factor wavelet transform," *Mechanical Systems and Signal Processing*, vol. 48, no. 1-2, pp. 103–119, 2014.
- [8] G. Yu, C. Li, and S. Kamarthi, "Machine fault diagnosis using a cluster-based wavelet feature extraction and probabilistic neural networks," *The International Journal of Advanced Manufacturing Technology*, vol. 42, no. 1-2, pp. 145–151, 2009.
- [9] J. Yan and L. Lu, "Improved Hilbert-Huang transform based weak signal detection methodology and its application on incipient fault diagnosis and ECG signal analysis," *Signal Processing*, vol. 98, pp. 74–87, 2014.
- [10] H. Demirel, C. Ozcinar, and G. Anbarjafari, "Satellite image contrast enhancement using discrete wavelet transform and singular value decomposition," *IEEE Geoscience and Remote Sensing Letters*, vol. 7, no. 2, pp. 333–337, 2010.
- [11] N. E. Huang, Z. Shen, S. R. Long et al., "The empirical mode decomposition and the Hilbert spectrum for nonlinear and non-stationary time series analysis," *Proceedings A*, vol. 454, pp. 903–995, 1998.
- [12] Z. H. Wu and N. E. Huang, "Ensemble empirical mode decomposition: a noise-assisted data analysis method," *Advances in Adaptive Data Analysis (AADA)*, vol. 1, no. 1, pp. 1–41, 2009.
- [13] Z. H. Wu and N. E. Huang, "A study of the characteristics of white noise using the empirical mode decomposition method," *Proceedings of the Royal Society A Mathematical, Physical and Engineering Sciences*, vol. 460, no. 2046, pp. 1597–1611, 2004.
- [14] N. Hu, M. Chen, G. Qin, L. Xia, Z. Pan, and Z. Feng, "Extended stochastic resonance (SR) and its applications in weak mechanical signal processing," *Frontiers of Mechanical Engineering in China*, vol. 4, no. 4, pp. 450–461, 2009.
- [15] X. Zhang, N. Hu, Z. Cheng, and L. Hu, "Enhanced detection of rolling element bearing fault based on stochastic resonance," *Chinese Journal of Mechanical Engineering*, vol. 25, no. 6, pp. 1287–1297, 2012.
- [16] F. Cong, J. Chen, and G. Dong, "Spectral kurtosis based on AR model for fault diagnosis and condition monitoring of rolling bearing," *Journal of Mechanical Science and Technology*, vol. 26, no. 2, pp. 301–306, 2012.
- [17] F. Combet and L. Gelman, "Optimal filtering of gear signals for early damage detection based on the spectral kurtosis," *Mechanical Systems and Signal Processing*, vol. 23, no. 3, pp. 652–668, 2009.

- [18] Y. Liu, B. He, F. Liu, S. Lu, and Y. Zhao, "Feature fusion using kernel joint approximate diagonalization of eigen-matrices for rolling bearing fault identification," *Journal of Sound & Vibration*, vol. 385, pp. 389–401, 2016.
- [19] C. Zhang, Z. Yin, X. Chen, and M. Xiao, "Signal overcomplete representation and sparse decomposition based on redundant dictionaries," *Chinese Science Bulletin*, vol. 50, no. 23, pp. 2672–2677, 2005.
- [20] R. A. Wiggins, "Minimum entropy deconvolution," *Geoexploration*, vol. 16, no. 1-2, pp. 21–35, 1978.
- [21] N. Sawalhi, R. B. Randall, and H. Endo, "The enhancement of fault detection and diagnosis in rolling element bearings using minimum entropy deconvolution combined with spectral kurtosis," *Mechanical Systems and Signal Processing*, vol. 21, no. 6, pp. 2616–2633, 2007.
- [22] H. Endo and R. B. Randall, "Enhancement of autoregressive model based gear tooth fault detection technique by the use of minimum entropy deconvolution filter," *Mechanical Systems and Signal Processing*, vol. 21, no. 2, pp. 906–919, 2007.
- [23] G. González, R. E. Badra, R. Medina, and J. Regidor, "Period estimation using minimum entropy deconvolution (MED)," *Signal Processing*, vol. 41, no. 1, pp. 91–100, 1995.
- [24] E. A. Robinson, S. Treitel, R. A. Wiggins, and P. R. Gutowski, *Digital seismic inverse methods*, International Human Resources Development Corp., Boston, Mass, USA, 1983.
- [25] P. Sharma, N. Sharma, and H. Sharma, "Elitism based Shuffled Frog Leaping algorithm," in *Proceedings of the 5th International Conference on Advances in Computing, Communications and Informatics, ICACCI 2016*, pp. 788–794, India, September 2016.
- [26] J.-Y. Lee and A. K. Nandi, "Extraction of impacting signals using blind deconvolution," *Journal of Sound and Vibration*, vol. 232, no. 5, pp. 945–962, 2000.
- [27] D. W. Eaton and J.-M. Kendall, "Improving seismic resolution of outermost core structure by multichannel analysis and deconvolution of broadband SmKS phases," *Physics of the Earth and Planetary Interiors*, vol. 155, no. 1-2, pp. 104–119, 2006.
- [28] G. F. Margrave, M. P. Lamoureux, and D. C. Henley, "Gabor deconvolution: Estimating reflectivity by nonstationary deconvolution of seismic data," *Geophysics*, vol. 76, no. 3, pp. W15–W30, 2011.
- [29] M. Bano, "Modeling and inverse Q imaging of ground penetrating radar waves in 1 and 2D," *Geophysical Research Letters*, vol. 23, no. 22, pp. 3123–3126, 1996.
- [30] J. Longbottom, A. Walden T, and E. White R, "Principles and application of maximum kurtosis phase estimation," *Geophysical Prospecting*, vol. 36, no. 2, pp. 115–138, 1988.
- [31] J. Zhao, M. Hu, H. Sun, and L. Lv, "Shuffled frog leaping algorithm based on enhanced learning," *International Journal of Intelligent Systems Technologies and Applications*, vol. 15, no. 1, pp. 63–73, 2016.
- [32] N. Rehman, C. Park, N. E. Huang, and D. P. Mandic, "EMD via MEMD: multivariate noise-aided computation of standard EMD," *Advances in Adaptive Data Analysis (AADA)*, vol. 5, no. 2, 2013.
- [33] P. Chen and T. Toyota, "Sequential fuzzy diagnosis for plant machinery," *JSME International Journal Series C Mechanical Systems, Machine Elements and Manufacturing*, vol. 46, no. 3, pp. 1121–1129, 2003.
- [34] D. Ho and R. B. Randall, "Optimisation of bearing diagnostic techniques using simulated and actual bearing fault signals," *Mechanical Systems and Signal Processing*, vol. 14, no. 5, pp. 763–788, 2000.



Hindawi

Submit your manuscripts at
www.hindawi.com

